

Article

The Clay Minerals in the Soils of the Gypseous Belt of Barbastro, NE Spain

Juan Herrero ^{1,*} , Raimundo Jiménez-Ballesta ²  and Carmen Castañeda ¹ 

¹ Estación Experimental de Aula Dei Consejo Superior de Investigaciones Científicas (CSIC), Ave. Montañana 1005, 50059 Zaragoza, Spain; ccastaneda@eead.csic.es

² Department of Geology and Geochemistry, Universidad Autónoma de Madrid, 28049 Madrid, Spain; profe.raimundojimenez@gmail.com

* Correspondence: jhi@eead.csic.es

Abstract: This article examines the clay mineralogy of twelve representative soils developed from gypsum-rich parent materials on several geomorphic positions. These soils were classified as Haploxerept, plus one profile as Humixerept and another as Xerorthent. The clay mineralogy, determined by X-ray diffraction, showed quite a similar clay composition in all profiles, with mica, chlorite, and smectite, from most to less abundant. Mica and chlorite are deemed inherited, while smectite—appearing in minor proportions—could result from both transformation and/or neoformation, because the leaching of bases by free drainage does not favor the transformation of mica to smectite. Therefore, the differences in clay mineralogy appeared to be lithogenic rather than pedogenic. These compositional data are an advance in the basic knowledge of the studied soils.

Keywords: gypseous soils; clay mineralogy; mica; chlorite; smectite; clay pedogenesis; weathering

1. Introduction

Gypsum ($\text{CaSO}_4 \cdot 2\text{H}_2\text{O}$) is the most known sulfate mineral and a common soil component in some regions of the world. The term “gypsiferous soils” was used by [1] for soils containing more than 2% gypsum. This term has a broader sense for [2], as “gypsiferous soils contain sufficient gypsum to influence soil physico-chemical, mineralogical, mechanical properties and geotechnical conditions and as a consequence, affect plant growth and crop production”. The word gypseous is better suited for soils having gypsum as the main component or as the responsible component for the main soil properties.

A sketch of the world presence of gypsum-rich soils and an estimation of their extent was made by [3] and [4], respectively. Most of these soils appear in arid countries, where the gypsum can persist in the soils due to the scanty rainfall and the limited solubility of gypsum in water (about 2.4 g L^{-1}), but they also occur in different climates like in Northern Russia [5], subboreal Eurasia [6], or Antarctica [7]. The gypsum-rich materials are problematic in civil engineering because of the subsidence and collapses when gypsum dissolves and because the waters containing sulfate corrode the iron and the standard concretes. Unlike soluble salts, gypsum does not stress the common crops; its limiting action is due to the low water storage capacity of gypsum-rich soils [8]. Moreover, the physicochemical effects of gypsum in soil due to its non-adherence to clay tactoids are very different from the cementing effects of calcite [9].

The present work studies the clay mineralogy of the soils developed on the outcropping nucleus of the Barbastro–Balaguer anticline, located in Ebro Basin, NE Spain (Figure 1). This outstanding landscape feature was first described as a gypseous belt “faja yesosa” by [10] and later studied by other geologists like [11–14], as well as by the geological maps of Instituto Geológico y Minero de España [15–17]. This belt, over 100 km long and between 2 and 10 km wide, is the outcrop of the gypseous Fm. Barbastro [18]. The belt stands out in the landscape because of its whitish color due to the gypsum abundance in soil, the



Citation: Herrero, J.; Jiménez-Ballesta, R.; Castañeda, C. The Clay Minerals in the Soils of the Gypseous Belt of Barbastro, NE Spain. *Land* **2024**, *13*, 1415. <https://doi.org/10.3390/land13091415>

Academic Editor: Cezary Kabala

Received: 12 August 2024

Revised: 29 August 2024

Accepted: 30 August 2024

Published: 2 September 2024



Copyright: © 2024 by the authors. Licensee MDPI, Basel, Switzerland. This article is an open access article distributed under the terms and conditions of the Creative Commons Attribution (CC BY) license (<https://creativecommons.org/licenses/by/4.0/>).

bald areas, and the limited aptness for agriculture and forestry [19]. The gypsophilous flora [20,21] allows the consideration of this area as an insular continental territory in the sense of [22]. All these circumstances support the interest of improving the knowledge of the soils on this gypseous outcrop.

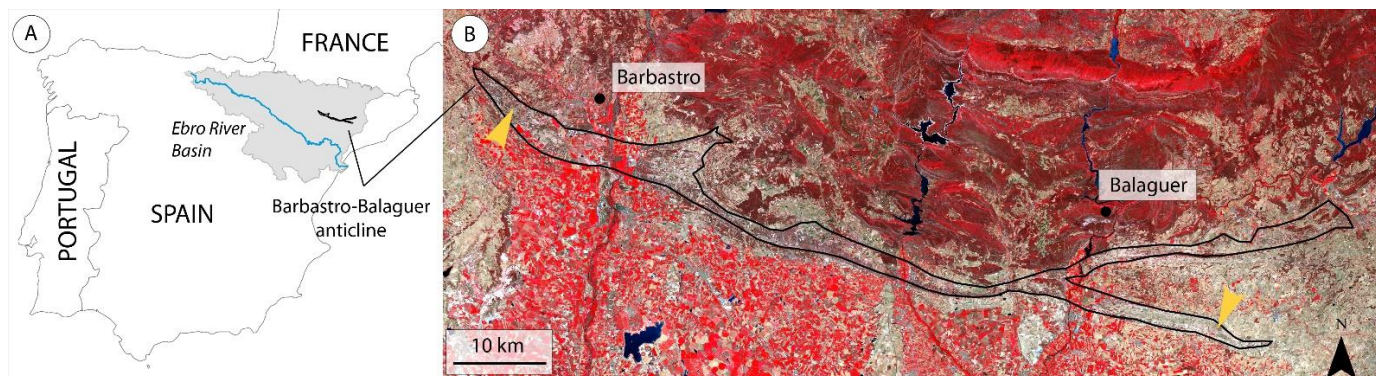


Figure 1. (A) Location of the Barbaastro gypsum outcrop within the Ebro Basin. (B) Delimitation of the outcropping Barbaastro–Balaguer anticline superimposed over a Sentinel-2 L2A false color composite (RGB 843) of 28 July 2024 downloaded from Sentinel Hub EObrowser (<https://www.sentinel-hub.com/explore/eobrowser/>, accessed on 31 August 2024). Yellow arrows point out the sampling areas.

Clays are key for the mechanical properties of soils, as well as for water and plant nutrient retention. Thus, the clay mineralogy of soils has been addressed in the literature for different types of parent rock, but rarely for gypseous ones, e.g., Egli et al. [23]. Our work is the first study on the clay mineralogy of the Barbaastro gypseous belt, whose soils undergo erosion and degradation associated with topographic and climatic factors, alongside changes in land use.

In this area, locally known as *chesa*, gypsum is ubiquitous in the soils [24,25]. The boundaries of the *chesa* against the surrounding lands are often well-contrasted, in terms of colors and vegetation. In the present article, the term “*chesas*” names the lands on the gypsum outcrop. The interest of the wildlife adapted to the local conditions led to the delineation within the *chesas* of an area covering 137 km² as the Special Conservation Area “ES2410074 Yesos de Barbaastro” (<http://natura2000.eea.europa.eu/Natura2000/SDF.aspx?site=ES2410074>, accessed on 31 August 2024) protected under the Habitats Directive of European Union. It is worth emphasizing that *chesa* soils are not saline, except for some scarce and distinct endorheic spots [26].

Wilson [27] stated that clay minerals record the pedogenetic history of soils, and extensive literature has studied the role of clays in soil behavior [28–32]. The review of clay mineralogy in Europe by [32] illustrates the drawbacks for mineralogical determinations due to the presence of gypsum.

Our examination of the clay mineralogy of the *chesa* contributes to the characterization of these soils, previous studies of which focused on their morphology and micromorphology [24,33]. The present article aims to find out: (i) what the main species of clay minerals present in these soils are, and (ii) the distribution patterns of clay minerals on the slopes of the *chesas*.

2. Material and Methods

2.1. Description of the Study Area

The most characteristic geomorphic features in the *chesas* are the hills with rounded shape and the flat-bottomed valleys, known with the name of *val* (plural form: *vales*). The bottom of most *vales* is cropped with winter cereal from immemorial times, and many of them have been terraced. Lateral gutters and berms are built in some *vales* as well. Often, erosion has incised the *val* with a longitudinal channel, or *tollo* by their local name. The *tollo* can be several meters deep, with vertical walls exposing the eroded materials that

filled the fossilized valleys carved by the erosion in the Quaternary. Table 1 uses some of these terms and others taken from [34] and lists, by their slope position, the studied profiles with the identifier number used by [24]. The sampling strategy was guided by the topographic positions (Table 1), and then two sampling areas were selected at the West and East ends of the gypsum outcrop, marked with arrows in Figure 1.

Table 1. Main features of the investigated soils (slope position, vegetation, and human intervention) and their classification after [35].

Slope Position/ ID	Aspect	Vegetation	Human Intervention	Classification
Saddle/135		<i>Q. faginea</i> , <i>Ononis tridentata</i>	Forest	Gypsic Haploxerept
Saddle/143		<i>Q. faginea</i> , <i>Q. coccifera</i> , <i>Rosmarinus officinalis</i> , <i>O. tridentata</i> , <i>Genista</i> sp., <i>Thymus</i> sp.	Degraded forest	Entic Humixerept
Header of val/22	W	Barley and almond trees	Terraces, plowing	Typic Haploxerept
Shoulder/143	N	<i>Q. faginea</i> , <i>Juniperus</i> sp., <i>Genista</i> sp.	Logging, thinning	Gypsic Haploxerept
Backslope/136	E	<i>Quercus coccifera</i> , lichens	Hunting	Lithic Xerorthent
Footslope/141	N	<i>Q. faginea</i> , <i>Q. coccifera</i> , <i>R. officinalis</i> , <i>Thymus</i> sp., <i>Genista</i> sp.	Very degraded forest	Gypsic Haploxerept
Footslope/151	N	<i>Q. faginea</i> , <i>Buxus sempervirens</i> , <i>R. officinalis</i> , <i>Lavandula</i> sp., moss	Degraded forest	Gypsic Haploxerept
Bottom of val/ 137	NE	Cereal	Terraces, lateral gutters, plowing	Gypsic Haploxerept
Bottom of val/ 138		<i>Q. faginea</i> , <i>Q. coccifera</i> , <i>Thymus</i> sp., <i>Genista</i> sp.	Plowing, abandoned crop	Gypsic Haploxerept
Bottom of val/ 140	NW	Barley stubble	Plowing	Gypsic Haploxerept
Cone of dejection from chesa/ 146		Cereal	Plowing	Gypsic Haploxerept
Alluvial plain from chesa/ 147		Cereal	Plowing	Fluentic Haploxerept

The main soil profile pattern of horizons is A-By-C, A-Bk-C, or A-C, after the designation of horizons by [35]. In general, the soil thickness increases from the summit to the toeslope, with maxima of >3 m in the dejection cone and the alluvial plain. The 60% of the soil colors described are 10YR, while 7.5YR are 25%, and 2.5Y are 10%. The most frequent soil structure was blocky and/or granular.

The Tamarite automatic weather station recorded for the period of 2003–2020 a mean annual rainfall of 337 mm/year, and a mean temperature of 14 °C, ranging between 12.2–14.7 °C. The mean evapotranspiration rate is 1027 mm/year, according to the Spanish network of agroclimatic stations (SIAR, Sistema de Información Agroclimática para el Regadío) of the Spanish Ministry of Agriculture. The soil temperature regime is deemed as thermic, and the moisture regime as xeric.

2.2. Mineralogical Analysis of Clays

Soil samples from horizons of different soils (Table 2) were air-dried and sieved to <2 mm Ø; 100 g of the sieved sample was then mixed with deionized water and disaggregated by agitation with glass balls. The flocculating action of the salts—in our case, the dissolved gypsum ubiquitous in the chesas—hampered the soil samples dispersion, as could be observed throughout the analyses of these soils. Chemical cementing agents (soluble salts, gypsum, carbonates, organic matter, and free iron forms) were eliminated prior to the separation of the clay fraction according to [36,37]. The <2 µm fraction was subsequently isolated by repeated siphoning of the dispersed material.

Table 2. Provenance of the soil samples for the presented clay analyses: profile identifier in [24], genetic horizon, XRD diagrams in oriented aggregates (OA), powder (P), ethylene glycol (EG), and heated (H). Last column is the page of the soil description in [24].

Profile Identifier	Horizon	XRD Diagrams	Page in [23]
22	Cy2	EG, H	310
134	Ay By	OA, EG OA, EG	126
135	A1 By	OA, EG OA, P	148
136	A1	OA, EG	120
137	By	OA, EG	194
138	By	OA, EG	192
140	By2	OA, EG	196
141	A1 Bk Cy	OA, EG OA, EG OA, EG	150
143	Ck	OA, EG	152
146	By2	EG, H	240
147	Ap Bw By	OA, EG OA, EG OA, EG	237
151	A1 Cy	OA, EG OA, EG	174

The clay study by X-ray diffractograms (XRD diagrams) in oriented aggregates and in samples treated with ethylene glycol were obtained with the methodology of [38]. The extraction was by successive decantation [39]. Organic matter was destroyed with 30% electrolytic peroxide H_2O_2 , while carbonates were eliminated with a buffered solution of sodic acetate/acetic acid at $pH > 4.2$. Gypsum was also eliminated to avoid flocculation that would interfere with the diffraction diagrams. For this purpose, a suspension of soil in a solution of NaCl 0.1N is shaken and filtered in a 50 μm mesh, discarding what is retained by the sieve. If needed, repeated siphoning was conducted until achieving a satisfactory dispersion. Then, the clays are saved by siphoning at the adequate depth and time according to Stokes law. The sodic clay is transformed to magnesian by exchange with $MgCl_2$ 1N.

The diffractometer used was a Philips with the radiation K_{α} ($\lambda = 0.179026$ nm) from cobalt filtered by an iron sheet. The excitation conditions were 35 KV and 18 mA, the time constant was 1 s, the exploration velocity $2^\circ/\text{min}$, the paper velocity 20 mm/min, the divergence slot 1° , and the reception slot 0.2 mm.

The minerals were identified with the ASTM Powder Diffraction File compiled by the Joint Committee on Powder and Diffraction Standards, as well as the works [39–42]. The primary minerals in selected samples were identified with diffractograms of unoriented powder. Diffractograms in oriented aggregates treated with ethylene glycol and in oriented aggregates were conducted on 45 soil samples for the identification of clay minerals. The differentiation between vermiculite and chlorite was carried out on selected samples heated at 500 $^\circ C$ for two hours.

3. Results

3.1. Clay Mineralogy

Figures 2–6 show XRD diagrams of the $<2 \mu m$ fraction in oriented aggregates, powder, or ethylene glycol, or heated for the selected twelve soil profiles. Table 2 lists the profiles

and horizons where the samples come from, maintaining the identifiers of [24]. For images of better quality, the reader is referred to <http://hdl.handle.net/10261/83011>, accessed on 11 August 2024.

The XRD diagrams repeatedly indicate the presence of three predominant minerals: micaceous clays (dioctahedral mica), chlorite, and small amounts of smectite. Chlorite and mica can be inherited from the parent material. The clay paragenesis is relatively similar for all horizons. Therefore, the soils of the study area retain most of the original soil components.

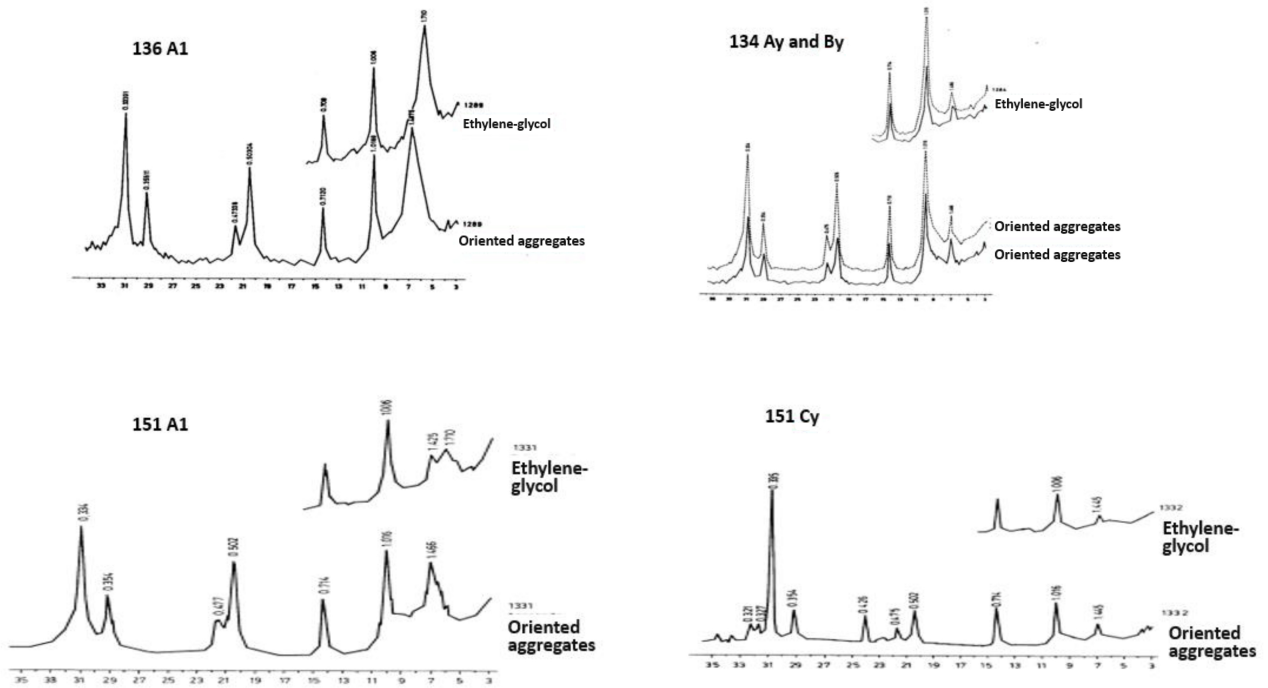


Figure 2. X-ray diffraction patterns of air-dried oriented aggregates and treated with ethylene glycol of clay fraction belonging to different horizons of profiles 136, 134, and 151.

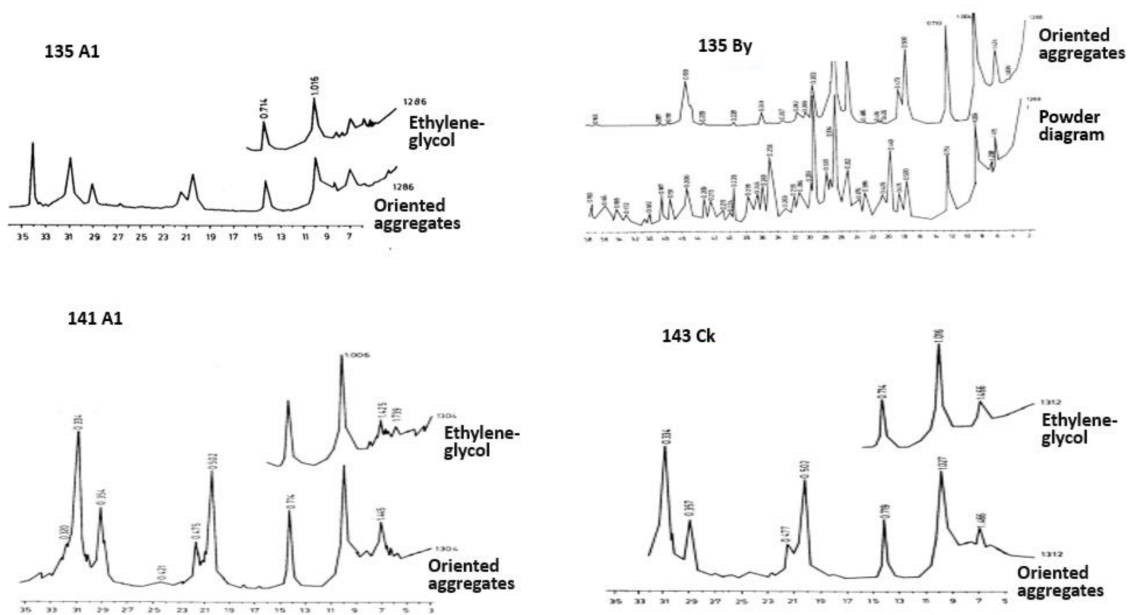


Figure 3. X-ray diffraction patterns of air-dried oriented aggregates and treated with ethylene glycol of clay fraction belonging to different horizons and profiles 135, 141, and 143.

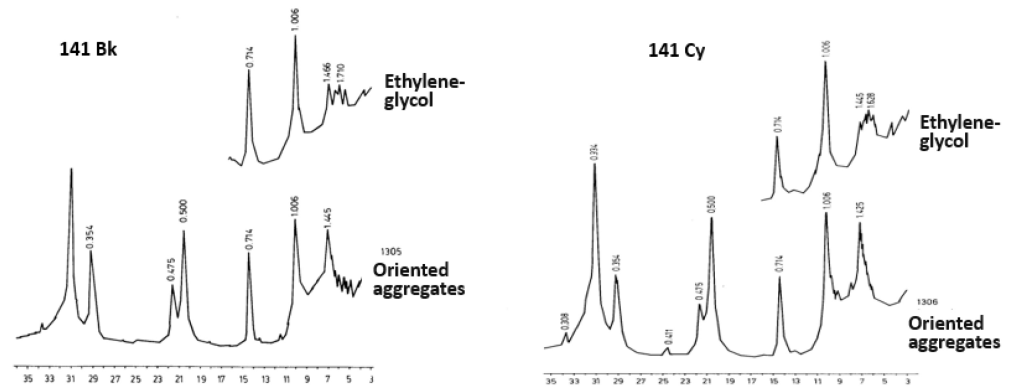


Figure 4. X-ray diffraction patterns of air-dried oriented aggregates and treated with ethylene glycol of clay fraction: variations with depth in the profile 141.

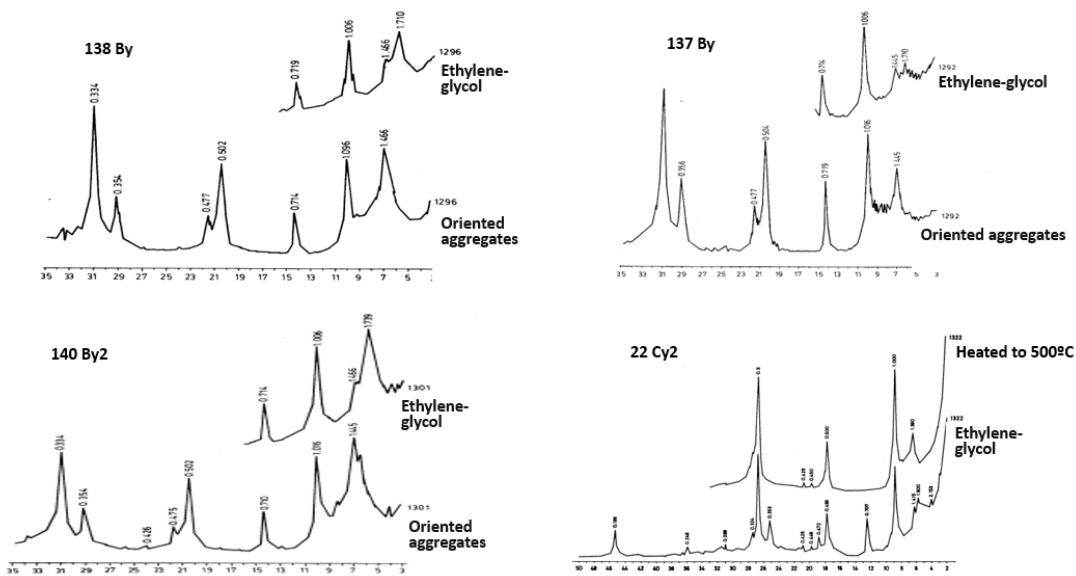


Figure 5. X-ray diffraction patterns of air-dried oriented aggregates, treated with ethylene glycol, and heated at 500 °C, of clay fraction belonging to different horizons and profiles 138, 137, 140, and 22.

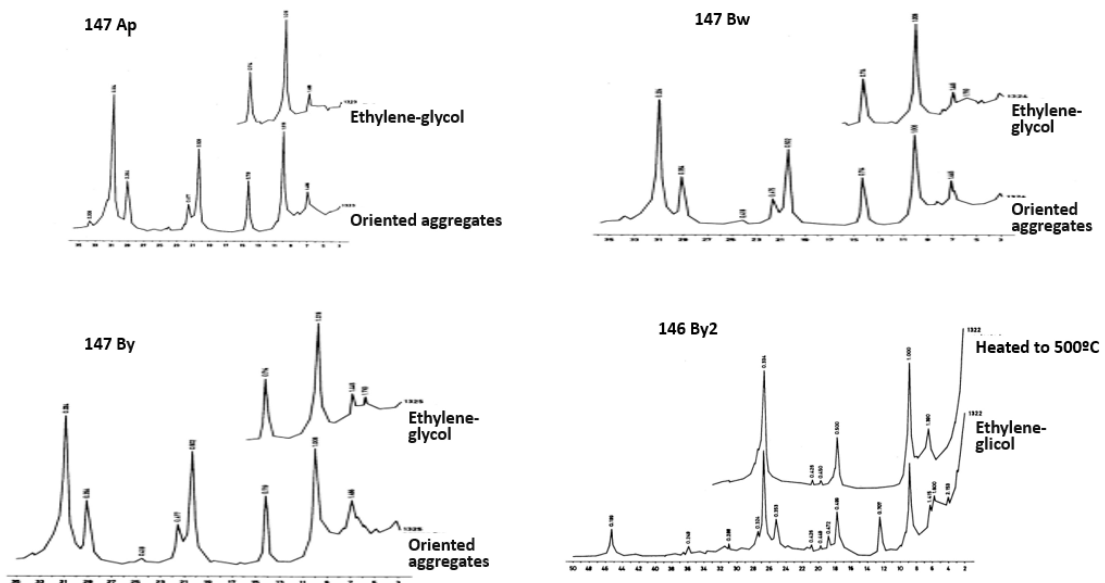


Figure 6. X-ray diffraction patterns of air-dried oriented aggregates, treated with ethylene glycol, and calcined at 500 °C, of clay fraction belonging to different horizons and profiles 147 and 146.

3.2. Mineralogy in Initial Stages of Pedogenesis (Protosoils)

Figure 2 shows the X-ray diffraction diagrams in oriented aggregates and in a sample treated with ethylene glycol, corresponding to the A1 horizon of the profile 136. The reflections at 1.001 stand out in the diffractogram of oriented aggregates, 0.503 and 0.335 nm corresponding to a dioctahedral mica. The reflections at 1.415 and 0.472 nm can be attributed to the smectite since the treatment with ethylene glycol makes the reflection at 1.415 nm disappear, while the one at 1.710 nm appears. The reflections at 0.705 and 0.354 nm are attributable to chlorite or vermiculite. The nonexistence of reflections at 1.052 and 0.540 nm, as well as those at 0.641, 0.450, and 0.320 nm, exclude the possibility of palygorskite.

3.3. Soils with Horizon of Microcrystalline Gypsum

The X-ray diffractograms from the profile 151 in oriented aggregates and in a sample treated with ethylene glycol are shown in Figure 2. The characteristic reflections of dioctahedral mica (1.001, 0.503, and 0.335 nm) are observed, as well as those of chlorite-vermiculite (1.415, 0.705, and 0.354 nm). A small amount of smectite also appears in the A horizon, as the reflection in the sample treated with ethylene glycol is of low intensity at 1.332 nm.

3.4. Soils on Slopes with Forest

Figure 2 also presents the X-ray diffractograms in oriented aggregates and in a sample treated with the ethylene glycol of the Ay and By horizons of the profile 134. In oriented aggregates, reflections at 1.001, 0.503, and 0.335 nm stand out, corresponding to a dioctahedral mica. The reflections at 1.415, 0.705, and 0.354 nm are attributable to chlorite or vermiculite. The presence of palygorskite can be excluded given the absence of the characteristic reflections (1.052, 0.641, 0.540, 0.450, and 0.320 nm).

In the soil profile 136, the clay composition was almost constant along the soil profile, which is attributed to the mineralogy of the parent material. As Hashemi [43] reported, pedogenesis in gypsiferous soils does not affect, essentially, the vertical distribution of the different clay species. In this case, the gypsiferous parent material was probably homogeneous. Only a slight increase is observed in the content of mica and trioctahedral chlorite in the surface horizon. This increase is interpreted as a result of the physical breakdown of coarse particles and/or of the preferential migration of other minerals; similar findings were reported by [44].

3.5. Soils with Calcic Endopedon in Poorly Erodible Positions

Figure 3 shows the X-ray diagrams of the profiles 135, 141, and 143, in powder, in oriented aggregates, in a sample treated with ethylene glycol, and in a sample heated at 500 °C, while Figure 4 shows variations with depth in the profile 141. The diffractograms show great similarity, with reflections corresponding to dioctahedral mica, chlorite-vermiculite, and some smectite. Smectite is present in the A1 horizon of pedon 135, although the reflection in the sample treated with ethylene glycol has very low intensity. In pedon 141, the smectite increases in depth, while, in 143, it is not abundant.

3.6. Soils in the Valley Bottoms

Figure 5 shows the X-ray diffraction diagrams in oriented aggregates and in samples treated with ethylene glycol from pedons 22, 137, 138, and 140. The reflections corresponding to the dioctahedral mica, as well as those of the chlorite-vermiculite, are present in all diagrams. The smectite content is low in all cases; in profiles 138 and 137 smectite increases in depth. The diagram of the sample heated at 500 °C maintains the reflection of 1.415 nm, showing that the effects attributable to chlorite-vermiculite in the diagrams of oriented aggregates correspond to chlorite. The absence of the characteristic reflections of palygorskite at 1.050 and 0.542 nm is also noteworthy in this case.

3.7. Soils in Plains Dominated by Chesas

Figure 6 shows the X-ray diagrams of the pedons 147 and 146 in powder, in oriented aggregates, in samples treated with ethylene glycol, and in samples heated at 500 °C. The diffractograms have the characteristic reflections of dioctahedral mica as well as those of chlorite-vermiculite, and those of smectite, the latter with low intensity. The mica presents high-intensity reflections at 0.503 nm compared to the reflection at 1.001, which allows us to affirm that it is a dioctahedral mica. As these are very acute effects, they correspond to little altered mica in most cases. Chlorite was present in all samples where heating was carried out to identify chlorite or vermiculite.

4. Discussion

The soils—generally located in dry areas—that contain sufficient quantities of gypsum to condition their behavior are named gypseous, and are well-represented in dry areas with sources of calcium sulfate. Topography influences the soils by their location in the slope and by their orientation, i.e., the sunny–shady effect. The soils of the chesas occur in rounded reliefs, in slopes, in valley bottoms, and in platforms. The soils studied here, located outside the chesas, have been formed on alluvial deposits from these.

The mineralogy of the studied soils showed little difference between topographic positions, although slight variations were detected probably due to internal drainage. The composition, properties, and minerals of the parent material, together with the topography and climate, control the intensity of weathering and erosion, and the resulting assemblage of phyllosilicates in soils of study area.

Semi-arid environments, as is the case of chesas, favor incomplete hydrolysis products of primary minerals, like illites and chlorites [45]. Thus, different factors must be considered such as erosional processes or the degree of acidity–basicity [46,47]. In semi-arid climates, gypseous materials barely generate complete hydrolytic processes, giving way to erosional processes [45,48]. Indeed, the primary composition of the parent materials is preserved despite the weathering processes. The weathering occurred under a semi-arid climate and the soil profiles were well-drained, with modest vegetation cover and often in unstable topographic positions, therefore with little edaphization.

The study of clay minerals in their own environment during soil formation has been widely investigated [28]. In this way, Wilson [27] reported that chlorite and illite (micaeous minerals) are believed to be largely inherited from parent rocks, with both minerals occurring commonly in areas where active mechanical erosion limits soil formation [49], which is the case for the chesas.

Three main sources of smectite in soils have been described: (1) neoformation from soil solution; (2) detrital origin or inheritance; and (3) transformation of other clay minerals. In this way, Borchardt [50] points out that low-lying topography, poor drainage, base-rich parent material, favorable chemical conditions characterized by a high pH, high silica activity, and an abundance of basic cations are the main factors influencing the origin and distribution of smectite in soils. Then, chesa soils probably provide favorable conditions for its formation. The smectite could be of detrital origin, but its non-uniform distribution allows us to discard such process. In calcareous arid and semi-arid soils, Khormali and Abtahi [51] stated that smectite is thought to be mainly of transformed origin.

What would be expected in our case is that the inheritance and transformation from illite are the main ways to explain the presence of smectite. However, this process does not seem to be well-developed, nor is the expected neoformation of palygorskite, a common mineral in gypsum soils after [52]. The neoformation of smectite was reported by [53]. Numerous studies have been carried out regarding clay mineralogy and weathering processes [28,46].

The preservation of appreciable amounts of mica, the absence of kaolinite, and the occurrence of the chlorite are indicative of not very intense weathering processes. Only the interpretation of the genesis of the small amounts of smectite should be approached critically, as this mineral can be either of detrital origin or it may be an alteration product. It is known that, during its formation, smectite inherits a significant compositional character

from the parent material. Smectite derived from muscovite is close to pure montmorillonite, as stated by Banfield and Eggleton [54]—“individual layers of K-depleted muscovite were probably converted to smectite”. Drainage conditions related to topography are a key factor in the transformation and redistribution of clay minerals in the soils of this region. The ubiquity and relative abundance of chlorite and mica are largely due to their presence in parent rocks, in such a way that the mineral composition of the soil reflects the evolutionary state of the soil, affected by various factors, with the nature of the parent material and the climate being the most important.

Globally speaking, the presence or absence of a certain mineral in the soil gives an idea about the formation and development of soil and the extent of the participation of its formation factors. In this way, the chlorite and mica minerals' presence and proportions respond fundamentally to the initial composition of the parental materials. The small proportions of smectite detected in several soil profiles require pedogenic processes.

The uncertainty about the mineral weathering and neosynthesis in arid soils referred to by [55] applies to chesá soils; on the other hand, the free infiltration in the chesás does not favor the formation and stability of smectite. Smectite in arid soils has been reported in Iraq [56], and Saudi Arabia [57,58]. For a semi-arid area, Omdí et al. [59] point out that clay mineral can be inherited from parent material—mainly illite and chlorite—but smectite can also result from illite under high-intensity weathering, and trioctahedral smectite and palygorskite can also result from neof ormation.

The present research identifies the clay minerals and their main source in soil, research that not only contributes to the recognition of the soil development process but also provides information for sustainable land management. Under natural conditions, the chesás bear vegetation covers, with the exception of sunny areas with a certain slope. Consequently, with vegetation cover, the surficial runoff is minimized and the erosion is uniform on the surface, even along the slopes. This is not the case in plowed areas, where rills are frequent despite the remediation measures taken by farmers.

In the chesás, most lichens occupy ecological niches with severe thermal, drought, and nutrient-scarcity conditions. They are pioneers in the colonization of these rocks, reaching a stage that sometimes stabilizes. This occurs in the steepest parts of the hills modeled in saccharoidal gypsum, especially at the southern exposures, where soil can barely develop. Crustacean lichens are also implanted on loose gypsum materials, prior to phanerogams, and on packages of farinaceous gypsum. The sunny areas and deforested areas with outcropping saccharoidal gypsum have steep slopes and hardly exceed the stage of muscinal colonization.

Rooting is preferentially initiated through dissolution cracks and in materials with a higher fine content; this entails a certain control of the vegetation by the outcropping strata and their inclination. The vertical circulation of water and subsequent dissolution are facilitated by the roots, which is why they are frequently associated with voids detected when hitting the surface of the soil with a hammer.

The valley bottoms are usually cultivated. Given their moderate longitudinal slopes or the frequent transversal terraces, the most apparent erosion is the gully incision—tollo by the local denomination—that acts as a collector in the rain episodes. However, the flat bottoms also undergo surface erosion, sometimes with gullies starting from a bald area, or also when a storm happens after the cereal harvesting.

Authors such as in [60] speculated that, generally, time controls the weathering development, and climate influences the dominant processes intensity, whereas the relief strongly influences the preservation/removal of the soil/regolith cover. In the chesás, as a semi-arid area, the most common soils are those with the absence or little development of the superficial A horizon. Our findings showed a mineral clay composition characterized by the presence of mica and chlorite which confirms their young pedogenetic stage of evolution. This agrees with the fact that the chemical weathering (hydrolysis) required for soil development is practically absent. In addition, erosion rates that quickly remove weathering products, plus the limited chemical alteration of bedrock, lead to shallow soils

with little development. These circumstances ought to be considered in the transformations to irrigation, whose shortcomings in gypsum-rich soils [61] must not be ignored in the irrigation schemes projected in the chesas.

From the knowledge gained, we are in a better position to understand the interaction between soil mineralogy and plants. Therefore, a future issue for administrative agencies is to use these data when setting priorities in relation to soils and their uses.

5. Conclusions

The clay mineralogy of soils developed on an outcrop of gypsum rocks in NE Spain was investigated to determine their origin and the factors controlling their distribution. The environmental conditions in the study area are not favorable to soil development, as reflected in the content and type of clay minerals present. Indeed, the soil profiles developed on gypsum from various landforms showed a mineral composition quite similar in all profiles: mica (dioctahedral), chlorite, and small amounts of smectite. The differences in clay mineralogy appeared to be lithogenic rather than pedogenic. Chlorite and mica abundance in soils is largely related to their presence in parent rocks; that is, these minerals are inherited. The primary minerals do not display chemical alteration; only smectite can be formed by alteration, because the good drainage of gypsum-rich soils might have hindered the transformation of mica to smectite.

The clay mineralogy is attributed to the fact that they are young soils developed from gypsum-rich parent material. Weak alterations generating low smectite contents could be considered indicators of subtle clay transformation in temperate gypseous soils. Since no further information is available on the clay mineralogy of the Barbastro gypsum belt, the results obtained reveal for the first time the general trend of its clays.

Author Contributions: J.H.: designed this study and collected the samples; R.J.-B. and J.H.: formal analysis and preparation of the draft; C.C.: draft review and editing, and funding acquisition. All authors have read and agreed to the published version of the manuscript.

Funding: This research was made possible by the grant PID2021-127170OB-I00 funded by MCIN/AEI/10.13039/501100011033 and by “ERDF A way of making Europe”, and the grant TED2021-130303B-I00 funded by MCIN/AEI/10.13039/501100011033 and by the “European Union NextGenerationEU/PRTR”.

Data Availability Statement: The original contributions presented in the study are included in the article, further inquiries can be directed to the corresponding author.

Conflicts of Interest: The authors declare no conflict of interest.

References

1. Van Alphen, J.G.; de los Ríos, F. *Gypsiferous Soils. Notes on Their Characteristics and Management*; Bulletin 12; International Institute for Land Reclamation and Improvement: Wageningen, The Netherlands, 1971; p. 44.
2. Pashaei, L.; Manafi, S.H. Characterization of gypsiferous soils in the north of Urmia, Iran. *Desert* **2021**, *26*, 1–15. [\[CrossRef\]](#)
3. Herrero, J.; Boixadera, J. Gypsic soils. In *Encyclopedia of Soil Science*; Lal, R., Ed.; Marcel Dekker Inc.: New York, NY, USA, 2002. [\[CrossRef\]](#)
4. Casby-Horton, S.; Herrero, J.; Rolong, N.A. Gypsum soils—Their morphology, classification, function, and landscapes. *Adv. Agron.* **2015**, *130*, 231–290. [\[CrossRef\]](#)
5. Goryachkin, S.V.; Spiridonova, I.A.; Sedov, S.N.; Targulian, V.O. Boreal soils on gypsum rocks: Morphology, properties, and genesis. *Eurasian Soil Sci.* **2003**, *36*, 691–703.
6. Yamnova, I.A.; Chernousenko, G.I. Gypsiferous Gazha Soils of the Subboreal Zone of Eurasia. *Eurasian Soil Sci.* **2023**, *56*, 1–15. [\[CrossRef\]](#)
7. Bockheim, J.G.; Ackert, R.P., Jr. Implications of soils on mid-Miocene-aged drifts in McMurdo Dry Valleys for ice sheet history and paleoclimate reconstruction. *Geomorphology* **2007**, *92*, 12–24. [\[CrossRef\]](#)
8. Moret-Fernández, D.; Herrero, J. Effect of gypsum content on soil water retention. *J. Hydrol.* **2015**, *528*, 122–126. [\[CrossRef\]](#)
9. Halitim, A.; Robert, M.; Berrier, J. Étude expérimentale de l’interaction de la calcite et du gypse avec la montmorillonite: Conséquences sur le rôle de ces deux minéraux dans le comportement de matériaux argileux et l’amendement des sols. *Comptes Rendus De L’académie Des Sci. De Paris Série II* **1983**, *296*, 1459–1464.
10. Mallada, L. *Descripción Física y Geológica de la Provincia de Huesca*; Facsimile edition; Instituto de Estudios Altoaragoneses: Huesca, Spain, 1878; p. 439. ISBN 978-84-86856-40-3.

11. Pardo, G.; Villena, J. Aportación a la geología de la región de Barbastro. *Acta Geol. Hisp.* **1979**, *14*, 289–292.
12. Sancho Marcén, C. Deformations associated with the Quaternary diapiric activity of the Barbastro Anticline, Huesca. *Cuaternario Y Geomorfol.* **1989**, *3*, 35–43. (In Spanish)
13. Lucha, P.; Gutiérrez, F.; Galve, J.P.; Guerrero, J. Geomorphic and stratigraphic evidence of incision-induced halokinetic uplift and dissolution subsidence in transverse drainages crossing the evaporite-cored Barbastro-Balaguer Anticline (Ebro Basin, NE Spain). *Geomorphology* **2012**, *171–172*, 154–172. [[CrossRef](#)]
14. Santolaria, P.; Ayala, C.; Pueyo, E.L.; Rubio, F.M.; Soto, R.; Calvín, P.; Luzón, A.; Rodríguez, A.; Oliván, C.; Casas, A.M. Structural and geophysical characterization of the western termination of the South Pyrenean triangle zone. *Tectonics* **2020**, *39*, e2019TC005891. [[CrossRef](#)]
15. Barnolas, A. (Director) *Memoria del Mapa Geológico de España, Escala 1:50000. Hoja 327, Os de Balaguer*; Instituto Geológico y Minero de España: Madrid, Spain, 2006; p. 74.
16. Barnolas, A. (Director) *Memoria del Mapa Geológico de España, Escala 1:50000. Hoja 287, Barbastro*; Instituto Geológico y Minero de España: Madrid, Spain, 2014; p. 40.
17. Barnolas, A. (Director) *Memoria del Mapa Geológico de España, Escala 1:50000. Hoja 326, Monzón*; Instituto Geológico y Minero de España: Madrid, Spain, 2017; p. 39.
18. Quirantes, J. *Estudio Sedimentológico y Estratigráfico del Terciario Continental de Los Monegros*; Institución “Fernando El Católico” Diputación Provincial de Zaragoza: Zaragoza, Spain, 1978; p. 208.
19. Olarieta, J.R.; Rodríguez-Ochoa, R.; Ascaso, E.; Antúnez, M. Rootable depth controls height growth of *Pinus halepensis* Mill. in gypsiferous and non-gypsiferous soils. *Geoderma* **2016**, *268*, 7–13. [[CrossRef](#)]
20. Ferrández-Palacio, J.V. Flora de una geografía diversa. In *Comarca de la Litera*; Palomares, A., Rovira, J., Eds.; Diputación General de Aragón: Zaragoza, Spain, 2008; pp. 27–38. ISBN 978-84-8380-142-0.
21. Mota, J.F.; Sánchez-Gómez, P.; Guirado, J.S. (Eds.) *Diversidad Vegetal de Las Yeseras Ibéricas. El Reto de Los Archipiélagos Edáficos para la Biología de la Conservación*; ADIF—Mediterráneo Asesores Consultores: Almería, Spain, 2011; p. 636.
22. Mota, J.F.; Martínez-Hernández, F.; Pérez-García, F.J.; Mendoza-Fernández, A.J.; Salmerón-Sánchez, E.; Merlo, M.E. Shipwrecked on the Rock, or Not Quite: Gypsophytes and Edaphic Islands. *Plants* **2024**, *13*, 970. [[CrossRef](#)] [[PubMed](#)]
23. Egli, M.; Plötze, M.; Tikhomirov, D.; Kraut, T.; Wiesenberg, G.; Lauria, G.; Raimondi, S. Soil development on sediments and evaporites of the Messinian crisis. *Catena* **2020**, *187*, 104368. [[CrossRef](#)]
24. Herrero, J. *Morfología y Génesis de Suelos Sobre Yesos*; n° 77; Monografías INIA: Madrid, Spain, 1991; p. 447.
25. Herrero, J.; Tierra, M.; Medina, E.T.; Castañeda, C. *Gypsum from Soils of Chesas, NE Spain*; Mendeley Data; Elsevier: Amsterdam, The Netherlands, 2024. [[CrossRef](#)]
26. Herrero, J.; Castañeda, C.; Velayos, M. Salada Farrachuela, a saline wetland in Tamarite de Litera, Spain. *Boletín De La Real Soc. Española De Hist. Nat.* **2020**, *114*, 67–80. [[CrossRef](#)]
27. Wilson, M.J. The origin and formation of clay minerals in soils: Past, present and future perspectives. *Clay Miner.* **1999**, *34*, 7–25. [[CrossRef](#)]
28. Velde, B.; Meunier, A. *The Origin of Clay Minerals in Soils and Weathered Rocks*; Springer: Berlin/Heidelberg, Germany, 2008; ISBN 978-3-540-75633-0.
29. Bonifacio, E.; Falson, G.; Simonov, G.; Sokolova, T.; Tolpeshta, I. Pedogenic processes and clay transformations in bisequal soils of the Southern Taiga zone. *Geoderma* **2009**, *149*, 66–75. [[CrossRef](#)]
30. Caner, L.; Joussein, E.; Salvador-Blanes, S.; Hubert, F.; Schlicht, J.F.; Duigou, N. Short-time clay-mineral evolution in a soil chronosequence in Oléron Island (France). *J. Plant Nutr. Soil Sci.* **2010**, *173*, 591–600. [[CrossRef](#)]
31. Watanabe, T.; Hasenaka, Y.; Hartono, A.; Sabiham, S.; Nakao, A.; Funakawa, S. Parent materials and climate control secondary mineral distributions in soils of Kalimantan, Indonesia. *Soil Sci. Soc. Am. J.* **2017**, *81*, 124–137. [[CrossRef](#)]
32. Yunta-Mezquita, F.; Van Liedekerke, M.; Fernández Ugalde, O.; Németh, T.; Balázs, R.B.; Keresztes, M.A.; Weiszburg, T.; Rábl, E.; Királyné Tóth, J.; Gazsi, Z.; et al. *Clay Mineral Inventory in Soils of Europe Based on LUCAS Survey Soil Samples*; Publications Office of the European Union: Luxembourg, 2024; JRC136950. [[CrossRef](#)]
33. Artieda, O.; Herrero, J. Pedogenesis in lutitic Cr horizons of gypsiferous soils. *Soil Sci. Soc. Am. J.* **2003**, *67*, 1496–1506. [[CrossRef](#)]
34. Schoeneberger, P.J.; Wysocki, D.A.; Benham, E.C. *Soil Survey Staff. Field Book for Describing and Sampling Soils, Version 3.0*; Natural Resources Conservation Service, National Soil Survey Center: Lincoln, NE, USA, 2021.
35. Soil Survey Staff. *Keys to Soil Taxonomy*, 13th ed.; USDA-Natural Resources Conservation Service: Washington, DC, USA, 2022.
36. Mehra, O.P.; Jackson, M.L. Iron oxide removal from soils and clay by dithionite-citrate system buffered with sodium bicarbonate. *Clays Clay Miner.* **1960**, *7*, 317–327. [[CrossRef](#)]
37. Kittrick, J.A.; Hope, E.W. A procedure for the particle-size separation of soils for X-ray diffraction analysis. *Soil Sci.* **1963**, *96*, 319–325. [[CrossRef](#)]
38. Robert, M. Principes de détermination qualitative des minéraux argileux à l’aide des rayons X. *Ann. Agron.* **1975**, *26*, 363–399.
39. Robert, M.; Tessier, D. Méthode de preparation des argiles des sols pour des études minéralogiques. *Ann. Agron.* **1974**, *25*, 859–882.
40. Kittrick, J.A.; Hope, E.W. A procedure for identification of small crystals by X-ray diffraction analysis. *Am. Mineral.* **1967**, *52*, 286–294.
41. Grim, R.C.; Bray, R.H.; Bradley, W.F. The mica in argillaceous sediments. *Am. Mineral.* **1937**, *22*, 813–819.

42. Brindley, G.W.; Brown, G. (Eds.) *Crystal Structures of Clay Minerals and Their X-ray Identification*; Mineralogical Society Monograph No. 5: London, UK, 1980. [[CrossRef](#)]
43. Hashemi, S.S.; Baghernejad, M.; Ghiri, M.N. Clay mineralogy of gypsiferous soils under different soil moisture regimes in Fars Province, Iran. *J. Agric. Sci. Technol.* **2013**, *15*, 1053–1068.
44. Van Ranst, E.; De Coninck, F.; Tavernier, R.; Langohr, R. Mineralogy in silty to loamy soils of central and high Belgium in respect to autochthonous and allochthonous materials. *Bull. De La Société Belg. De Géologie* **1982**, *91*, 27–44.
45. Curtis, C.D. Aspects of climatic influence on the clay mineralogy and geochemistry of soils, palaeosols and clastic sedimentary rocks. *J. Geol. Soc.* **1990**, *147*, 351–357. [[CrossRef](#)]
46. Kasanin-Grubin, M. Clay mineralogy as a crucial factor in badland hillslope processes. *Catena* **2013**, *106*, 54–67. [[CrossRef](#)]
47. Barré, P.; Fernández-Ugalde, O.; Virto, I.; Velde, B.; Chenu, C. Impact of phyllosilicate mineralogy on organic carbon stabilization in soils: Incomplete knowledge and exciting prospects. *Geoderma* **2014**, *235–236*, 382–395. [[CrossRef](#)]
48. Chorom, M.; Rengasamy, P.; Murray, R.S. Clay dispersion influenced by pH and net particle charge of sodium soils. *Aust. J. Soil Res.* **1994**, *32*, 1243–1252. [[CrossRef](#)]
49. Fanning, D.S.; Keramidas, V.Z.; El-Desoky, M.A. Micas. In *Minerals in Soil Environment*; Dixon, J.B., Weed, S.B., Eds.; Soil Science Society of America: Madison, WI, USA, 1989; pp. 551–634.
50. Borchardt, G. Smectites. In *Minerals in Soil Environment*; Dixon, J.B., Weed, S.B., Eds.; Soil Science Society of America: Madison, WI, USA, 1989; pp. 675–727.
51. Khormali, F.; Abtahi, A. Origin and distribution of clay minerals in calcareous arid and semi-arid soils of Fars Province, southern Iran. *Clay Miner.* **2003**, *38*, 511–527. [[CrossRef](#)]
52. Khademi, H.; Mermut, A.R. Source of palygorskite in gypsiferous Aridisols and associated sediments from central Iran. *Clay Miner.* **1998**, *33*, 561–578. [[CrossRef](#)]
53. Gharaee, H.A.; Mahjoory, R.A. Characteristics and geomorphic relationships of some representative aridisols in Southern Iran. *Soil Sci. Soc. Am. J.* **1984**, *48*, 1115–1119. [[CrossRef](#)]
54. Banfield, J.F.; Eggleton, R.A. Analytical transmission electron microscope studies of plagioclase. Muscovite and K-feldspar weathering. *Clays Clay Miner.* **1990**, *38*, 77–89. [[CrossRef](#)]
55. Boettinger, J.L.; Southard, R.J. Phyllosilicate distribution and origin in Aridisols on a granitic pediment, Western Mojave Desert. *Soil Sci. Soc. Am. J.* **1995**, *59*, 1189–1198. [[CrossRef](#)]
56. Al-Rawi, A.H.; Jackson, M.L.; Hole, F.D. Mineralogy of some arid and semiarid land soils of Iraq. *Soil Sci.* **1969**, *107*, 480–486. [[CrossRef](#)]
57. Aba-Husayn, M.M.; Dixon, J.B.; Lee, S.Y. Mineralogy of Saudi Arabian soils: Southwestern region. *Soil Sci. Soc. Am. J.* **1980**, *44*, 643–649. [[CrossRef](#)]
58. Lee, S.Y.; Dixon, J.B.; Aba-Husayn, M.M. Mineralogy of Saudi Arabian Soils: Eastern Region. *Soil Sci. Soc. Am. J.* **1983**, *47*, 321–326. [[CrossRef](#)]
59. Omdi, F.E.; Daoudi, L.; Fagel, N. Origin and distribution of clay minerals of soils in semi-arid zones: Example of Ksob watershed (Western High Atlas, Morocco). *Appl. Clay Sci.* **2018**, *163*, 81–91. [[CrossRef](#)]
60. Derakhshan-Babaei, F.; Nosrati, K.; Tikhomirov, D.; Christl, M.; Sadough, H.; Egli, M. Relating the spatial variability of chemical weathering and erosion to geological and topographical zones. *Geomorphology* **2020**, *363*, 107235. [[CrossRef](#)]
61. Herrero, J. On the early irrigation of gypseous lands in Spain. *Land Degrad. Dev.* **2017**, *28*, 1152–1155. [[CrossRef](#)]

Disclaimer/Publisher’s Note: The statements, opinions and data contained in all publications are solely those of the individual author(s) and contributor(s) and not of MDPI and/or the editor(s). MDPI and/or the editor(s) disclaim responsibility for any injury to people or property resulting from any ideas, methods, instructions or products referred to in the content.